Features of the Phase Fluctuation Structure of a Laser Beam in a Turbulent Medium

A. M. Zotov[*], E. G. Kim[**], P. V. Korolenko[***], and P. P. Solopov[****]

Faculty of Physics, Lomonosov Moscow State University, Leninskie Gory 1, str. 2, Moscow, 119991 Russia

Abstract—A method for reconstruction of the laser beam phase from shearing interferograms using separation of the amplitude and phase parts of the spatial spectrum is proposed and tested both numerically and experimentally with a laboratory model of the turbulent atmosphere, which allows purposefully varying the state of turbulence and controlling its parameters. Amplitude-phase correlation in the fluctuation structure of the laser beam that passed through turbulent medium is investigated. The recorded correlation coefficient typical of weak fluctuations varies in the range of 0.2 to 0.3.

1. INTRODUCTION

Formation of a fluctuation structure of laser beams was theoretically and experimentally investigated in a number of works [1, 2]. However, investigations of the phase fluctuation structure are much fewer in number than investigations of intensity fluctuations, largely due to an appreciably more complicated procedure for detection of variations in the light oscillation phase and necessity to have instruments specially adapted to this kind of measurement [3]. Nevertheless, it is impossible to comprehend the radiation properties without the information on the phase because it is the variation in the spatial phase distribution that dictates the dynamics of the variation in the beam intensity profile in the turbulent medium. Among the phase detection methods in use, shearing interferometry is worth noting, which allows phase and intensity fluctuations to be detected in parallel. The main advantages of this method are technical simplicity and availability of optical elements. However, its practical use requires optimization of the shearing interferometer parameters, suppression of the noise in the radiation, and development of the techniques of interference pattern processing.

Approaches to the processing of shearing interferograms and relevant algorithms are considered in [4], but in practice these algorithms do not always ensure the necessary phase detection accuracy in both static and dynamic regimes. In this work, we consider possibilities of improving the procedure for detection of phase variations in the laser beam cross section by constructing new algorithms based on separation of the intensity and phase data using spectral spatial filters and subsequent reconstruction of the desired distributions using the deconvolution method.

2. EXPERIMENTAL SETUP AND MEASUREMENT PROCEDURE

The amplitude-phase fluctuations of the radiation were investigated using a setup described in detail in [5]. Its operation was based on multiple passage of the laser beam at the wavelength $\lambda = 532$ nm with the Gaussian intensity distribution through a special cell with a turbulent medium produced by mixing cold and hot air flows. The intensity of the turbulent processes could vary with the rate and temperature of the flows.

The phase fluctuation distribution data for the laser beams that passed through the turbulent medium were obtained using a shearing interferometer, which was a glass plate with the surfaces inclined at small angles. The light beams reflected from the front and rear surfaces of the plate turned out to be transversely shifted with respect to each other. As a result of their relative inclination, a lateral shear interference pattern was formed, which was recorded by a high-speed (400 FPS) camera. The video images were transmitted to the computer for processing. An example of a lateral shear interferogram obtained in the experiment is shown in Fig. 1(a).

Note that the plane-parallel plate should have a wedge angle such as to maximize the number of fringes distinguishable on the CCD matrix. Maxi-

[*]E-mail: `azotov@gmail.com`
[**]E-mail: `kim.elena@physics.msu.ru`
[***]E-mail: `pvkorolenko@rambler.ru`
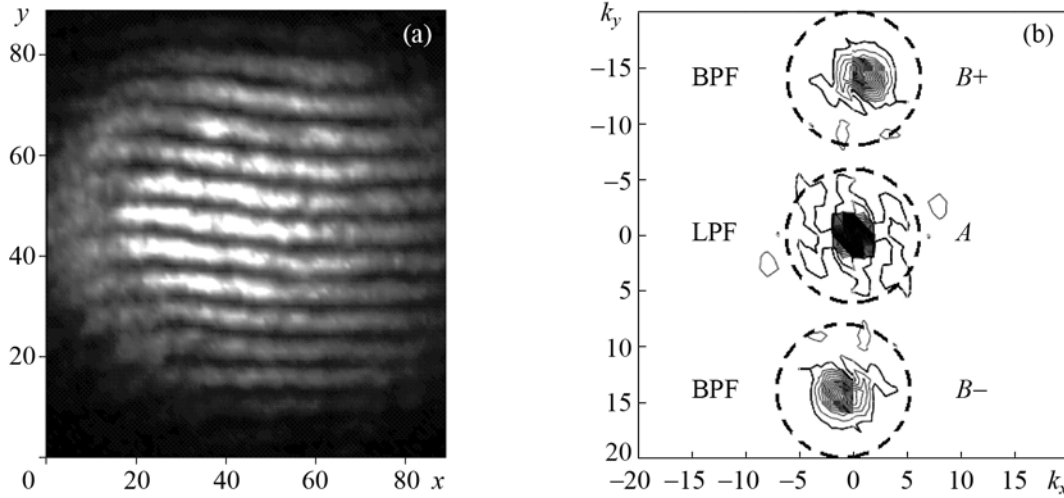[****]E-mail: `petr.neonov@gmail.com`

Fig. 1. Shearing interferogram obtained in the experiment (a) and its spatial spectrum (b); A, $B+$, and $B-$ are the components of the spatial spectrum; positions of spectral filters are shown by dashed circles; X and Y are the spatial coordinates.

mization of the number of fringes entails the largest spatial separation of the spectral components and rules out their overlapping. If the scale of the intensity inhomogeneities is close to the period of the interference fringes, the interferogram processing will yield only qualitative results.

3. DESCRIPTION OF THE ALGORITHM FOR RECONSTRUCTION OF WAVE INTENSITY AND PHASE

The interferogram processing is based on that the intensity and phase information in the spatial spectra is separated in the case of weak turbulence, when the fringes are continuous and the wave front has no topological distortions. Thus, if the amplitude-phase profile of the beam is not heavily distorted, it becomes possible to separate the information on the phase and intensity using spectral spatial low-pass and band-pass filters (LPFs and BPFs) and considerably simplify the phase reconstruction problem, which in the general case is classified as an ill-posed problem [4].

The processing of the shearing interferogram thus results in obtaining the data on the phase shift of the sheared beams and on the sum of their intensities at particular points of the interferogram. Then the phase distribution found from the phase shift and the intensity distribution found from the sum of the intensities can be reconstructed using the deconvolution method.

We consider in more detail the algorithm for the reconstruction of the light beam intensity and phase. Let the wave reflected from two surfaces of the plate be incident on the screen. The intensity distribution of the shearing interferogram on the screen is described by the formula

$$I_{int}(\mathbf{r}) = \underbrace{I(\mathbf{r}) + \beta^2 I(\mathbf{r}-\Delta\mathbf{r})}_{A}$$
$$+ \underbrace{2\sqrt{I(\mathbf{r})\,\beta^2 I(\mathbf{r}-\Delta\mathbf{r})}\cos\left[\varphi(\mathbf{r}) - \varphi(\mathbf{r}-\Delta\mathbf{r}) + \mathbf{n}\mathbf{r}\right]}_{B} \quad (1)$$

with expressions A and B carrying information on the intensity and the phase, respectively. In the above formula, $\mathbf{r}$ is the radius vector of the position of the point in the image, $I_{int}(\mathbf{r})$ is the intensity distribution in the shearing interferogram, $I(\mathbf{r})$ is the desired intensity distribution of the beam incident on the interferometer, β is the amplitude attenuation factor for the beam reflected from the rear surface of the plane-parallel plate, $\varphi(\mathbf{r})$ is the desired phase distribution of the beam before passing through the interferometer, $\Delta\mathbf{r}$ is the radius vector of the relative shift of the beam reflected from the rear surface of the plate measured in pixels, $\mathbf{n} = (2\pi N_x/L, 2\pi N_y/L)$ is the radius vector characterizing inclination of two reflecting surfaces of the plate and accordingly inclination of the fringes, where L is the maximum field size measured in pixels, and N_x and N_y are the numbers of intersections of the fringes with the horizontal and vertical lines.

The auxiliary parameters β^2 and $\Delta\mathbf{r}$ are easily obtained by passing the beam thorough a narrow round diaphragm and estimating the intensity ratio and the relative shift of its images.

Let us describe some auxiliary functions and transformations needed for processing interferograms. The spectral filters $LPF(\mathbf{k})$ and $BPF(\mathbf{k})$ are given in the form of super-Gaussian functions with the center in the middle of the spatial spectrum and at the centers of the regions where the interference fringe spectra are localized (hereinafter $\mathbf{k}$ is the vector denoting spatial frequencies).

The LPF(**k**) and BPF(**k**) filters are tuned to cover the main part of the spectrum. The LPF passes the spectrum of characteristic intensity inhomogeneity scales that corresponds to expression A in (1), and the BPF is tuned to the average frequency of the fringes that correspond to expression B in (1). Figure 1(b) shows the structure of the spatial spectrum of the shearing interferogram and the arrangement of the filters, the LPF(**k**) and the two-component symmetrical BPF(**k**).

In what follows we will use fast 2D Fourier transform designated as $\mathcal{F}\{\ \}$; the region of negative frequencies can be obtained using the range where $k_x, k_y > L/2$ with $k_x = \mathrm{mod}(k_x + L/2, L) - L/2$ and $k_y = \mathrm{mod}(k_y + L/2, L) - L/2$. We will also assume that frequencies close to $L/2$ (on the order of the Nyquist frequency) have negligibly low amplitudes.

First, we consider the intensity reconstruction procedure. After the spectral filtration of the intensity distribution $I_{\mathrm{int}}(\mathbf{r})$ using the LPF we have

$$\mathrm{LPF}(\mathbf{k})\,\mathcal{F}\{I_{\mathrm{int}}(\mathbf{r})\} \cong \mathcal{F}\{I(\mathbf{r}) + \beta^2 I(\mathbf{r}-\Delta\mathbf{r})\}. \quad (2)$$

The right-hand side of (2) is a sum of the intensities of the beam and its copy shifted by $\Delta\mathbf{r}$, and we can therefore rewrite it as a convolution

$$I_{\mathrm{int}}^{\mathrm{LPF}}(\mathbf{r}) = \int I(\mathbf{p})\,G_I(\mathbf{r} - \mathbf{p})\,d\mathbf{p}, \quad (3)$$

where the convolution kernel $G_I(\mathbf{r}) = \delta(\mathbf{r}) + \beta^2 \delta(\mathbf{r} - \Delta\mathbf{r})$ has the form of an $L{\times}L$ matrix with its elements equal to unity if $\mathbf{r} = (0,0)$, β^2 if $\mathbf{r} = \Delta\mathbf{r}$, and zero in all other cases.

If we solve the deconvolution problem in the spectral representation, the spectral filtration and deconvolution operations can be united, which allows two (direct and inverse) intermediate Fourier transforms to be eliminated. Then, introducing the Wiener filter W that depends on $\mathbf{k}$ in the general case, we obtain

$$I(\mathbf{r}) = \mathcal{F}^{-1}\left\{\frac{\mathrm{LPF}(\mathbf{k})\,\mathcal{F}\{I_{\mathrm{int}}\}\,\overline{\mathcal{F}\{G_I\}}}{\mathcal{F}\{G_I\}\,\overline{\mathcal{F}\{G_I\}} + W}\right\}. \quad (4)$$

Here $\overline{\mathcal{F}\{G_I\}}$ means complex conjugation.

Now we turn to the phase reconstruction procedure to be performed in several steps.

Step 1. Using the symmetrical BPF, we separate those parts of the spatial spectrum which determine the structure of the interference fringes

$$\mathrm{BPF}(\mathbf{k})\,\mathcal{F}\{I_{\mathrm{int}}(\mathbf{r})\} \cong \mathcal{F}\Big\{2\beta\sqrt{I(\mathbf{r})\,I(\mathbf{r}-\Delta\mathbf{r})}$$
$$\times \cos\big[\varphi(\mathbf{r}) - \varphi(\mathbf{r}-\Delta\mathbf{r}) + \mathbf{nr}\big]\Big\}. \quad (5)$$

Step 2. Using the two-dimensional analogue of the Hilbert transform [6, 7] and eliminating negative frequencies by choosing one of the spectral components $B+$ or $B-$ (see Fig. 1(b)) we go, in view of (5), to the expression

$$P(\mathbf{r}) = 2\beta\sqrt{I(\mathbf{r})\,I(\mathbf{r}-\Delta\mathbf{r})}$$
$$\times \exp\Big\{i\big[\varphi(\mathbf{r}) - \varphi(\mathbf{r}-\Delta\mathbf{r}) + \mathbf{nr}\big]\Big\}. \quad (6)$$

The choice of positive frequencies results from choosing the "+" sign for **n**. Taking the argument from (6), we find the quantity $\varphi(\mathbf{r}) - \varphi(\mathbf{r}-\Delta\mathbf{r}) + \mathbf{nr}$ defined on the interval $(-\pi, \pi)$.

Step 3. To obtain a continuous phase distribution, we join phase discontinuities, first in the direction of the fastest increase in the number of fringes, e.g., X when $N_x > N_y$, and then in the perpendicular direction. Next, subtracting the linear part **nr** related to the constant average inclination of the fringes, we obtain an expression for the phase shift

$$f(\mathbf{r}) = \varphi(\mathbf{r}) - \varphi(\mathbf{r}-\Delta\mathbf{r}). \quad (7)$$

Step 4. To obtain the phase distribution, we use deconvolution

$$f(\mathbf{r}) = \int \varphi(\mathbf{p})\,G_\varphi(\mathbf{r} - \mathbf{p})\,d\mathbf{p}, \quad (8)$$

where the convolution kernel

$$G_\varphi(\mathbf{r}) = \delta(\mathbf{r}) - \delta(\mathbf{r} - \Delta\mathbf{r}) \quad (9)$$

is an $L{\times}L$ matrix with the elements equal to 1 if $\mathbf{r} = (0,0)$, -1 if $\mathbf{r} = \Delta\mathbf{r}$, and 0 in all other cases. Now using the convolution theorem, we can obtain the desired phase distribution from the expression

$$\varphi(\mathbf{r}) = \mathcal{F}^{-1}\left\{\frac{\mathrm{LPF}(\mathbf{k})\,\mathcal{F}\{f\}\,\overline{\mathcal{F}\{G_\varphi\}}}{\mathcal{F}\{G_\varphi\}\,\overline{\mathcal{F}\{G_\varphi\}} + W}\right\}. \quad (10)$$

The LPF is used here for obtaining a spatial spectrum of frequencies in the same region as for the intensity.

Note that in the phase reconstruction method described above the phase is reconstructed accurate to a constant value. This is however insignificant since most often it is needed to know phase variations. It should also be borne in mind that the shearing interferometry results are incomplete if the shearing direction coincides with the direction of the "folds" of the wave front of the beam under investigation. In the latter case, we can speak about the zero average phase effect along the beam shearing direction.

Thus, having independent distributions of intensity (4) and phase (10), we can investigate correlations in the light beam intensity and phase variations.
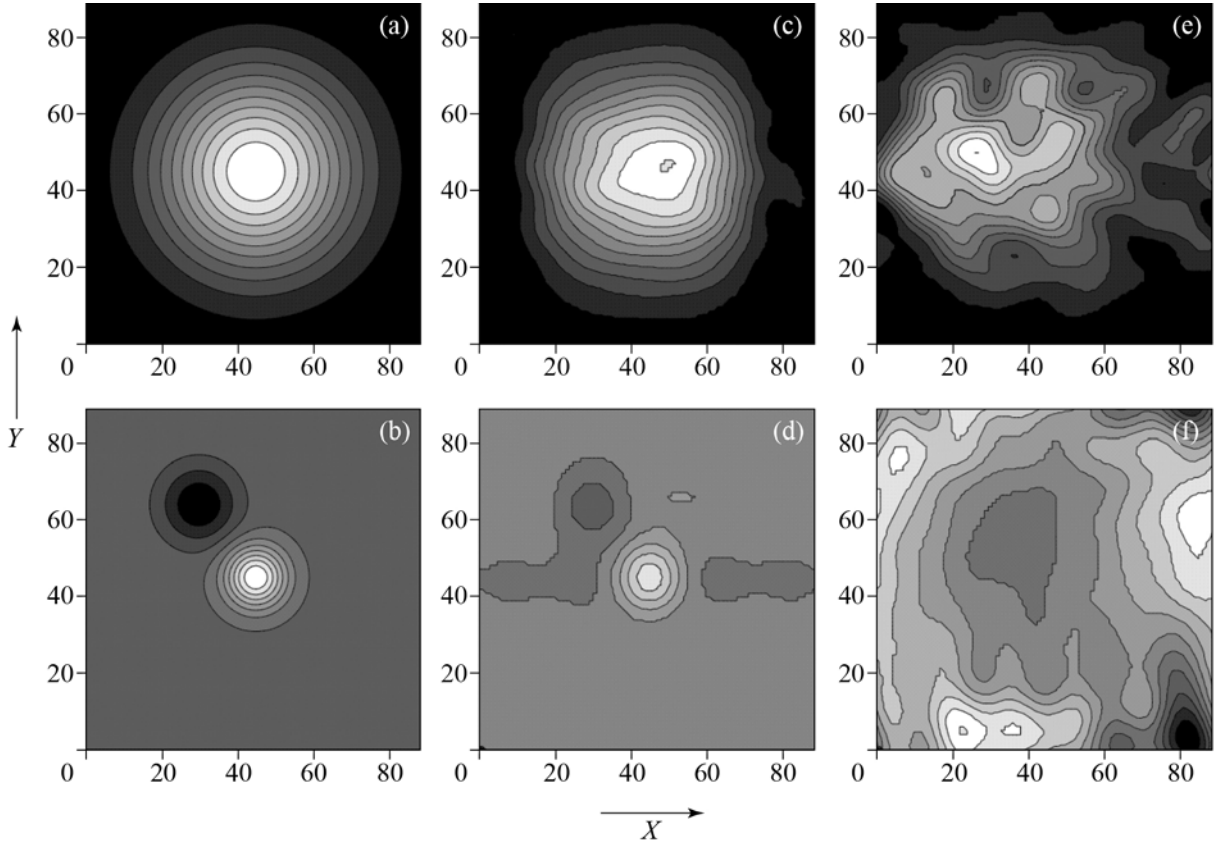
Fig. 2. Model and experimental intensity and phase distributions. (a) Gaussian intensity distribution (model), (b) wave front distortions (model), (c, d) intensity and phase distributions reconstructed from the model interferogram, and (e, f) intensity and phase distributions reconstructed from the real interferogram (see Fig. 1(a)). The X and Y coordinates are presented in relative units.

4. TESTING RESULTS AND EXPERIMENTAL DATA

Let us numerically test the above phase reconstruction method. As a test light structure, we choose a Gaussian beam with two bell-like wave front distortions π and $-\pi/2$ high. The intensity and phase of this beam are given by the expressions

$$I(\mathbf{r}) = \exp\left(\frac{|\mathbf{r} - \mathbf{c}|^2}{25^2}\right), \qquad (11)$$

$$\varphi(\mathbf{r}) = \pi \exp\left(\frac{|\mathbf{r} - \mathbf{c}|^2}{8^2}\right)$$
$$- \frac{\pi}{2} \exp\left(\frac{|\mathbf{r} - \mathbf{c} - \overrightarrow{(15, -19)}|^2}{10^2}\right), \quad (12)$$

where $\mathbf{c}$ is the radius vector of the screen center position. The shift of the beams $\Delta\mathbf{r}$ in the interferogram plane is determined by the radius vector $(16, 1)$, the numbers of the fringes in the horizontal and vertical directions are $N_x = 1$ and $N_y = 17$, and the coefficient β^2 is 0.82 (these parameters correspond to the experimental conditions). Intensity and phase distributions (11) and (12) of the tested beam are plotted in Figs. 2(a,b). Constructing a shearing interferogram that corresponds to the test beam structure and applying to it the above-described phase and intensity reconstruction procedure, we obtain distributions presented in Figs. 2(c,d). As is evident from the figures, the reconstructed wave front generally follows the profile of the original one; a slight difference of the reconstructed phase distribution from the initial one is due to the zero average phase effect along the beam shearing direction in the interferometer.

The above approach was also applied to the processing of the shearing interferograms obtained directly in the experiment. Here are the data related to the interferogram shown in Fig. 1(a). It corresponds to the regime of a weakly turbulent medium in a multipass cell. Processing of a real interferogram requires considering the effect of the negative factors that arise first of all from the noisiness of the light field. When the noise of the image is comparable with the visibility of the fringes, uncertainty appears in the estimation of the phase values. This is manifested first of all at the periphery of the field under processing. Unlike the case with intensity, which is smoothly brought to zero at the periphery of the distribution (physically or by
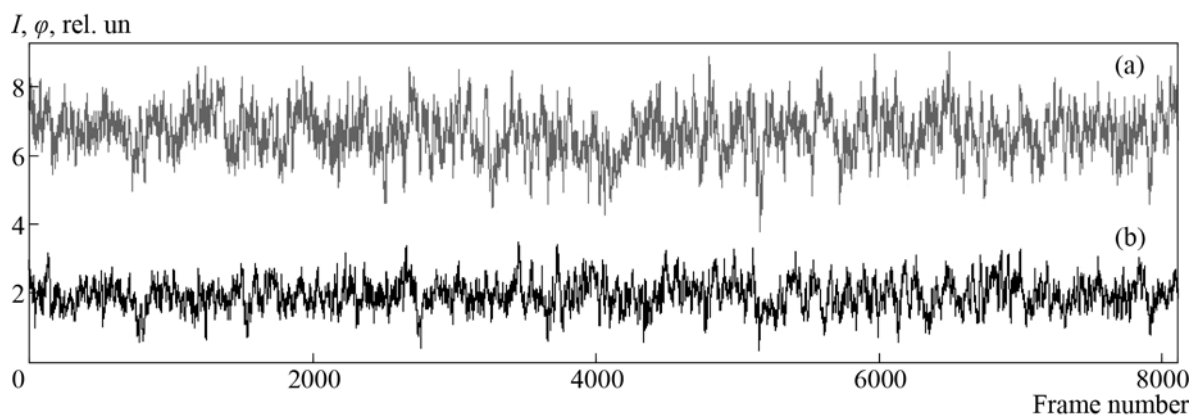
Fig. 3. Local temporal fluctuations of intensity I (a) and phase φ (b). The correlation factor is 0.3.

software), the choice of the preferable phase value is not obvious. Changing over to a narrower aperture does not solve the problem since this complicates phase joining related to the cyclicity of the Fourier method at the boundaries of the image. The intensity and phase distributions obtained from the processing of the interferogram are presented in Figs. 2(e,f). Since the transmission beam was only slightly distorted due to weak turbulence of the medium, the beam intensity profile has a near-Gaussian bell-like shape, as is seen in Fig. 2(e). The phase distribution (Fig. 2(f)) is close to homogeneous at the center of the beam while at the periphery considerable perturbations of the phase structure occur for the above-mentioned reason.

On processing a series of shearing interferograms, we obtained data on local temporal variations in phase and intensity. Temporal fluctuations of intensity and phase for the weak turbulence regime are shown in Fig. 3. Though fluctuations of intensity and phase are generally different in character, there is certain similarity in their variations. The intensity and phase correlation factors for the near diffraction region calculated from the experimental data varied between 0.2 and 0.3. This correlation reflects the initial formation stage of the amplitude-phase profile of the beam that passed through the turbulent medium.

5. CONCLUSIONS

The developed method for determining amplitude-phase characteristics of laser beams that passed through a turbulent medium from the shearing interferograms allows the information on the intensity and phase fluctuations to be effectively separated. This makes the algorithms for the reconstruction of the intensity and phase distributions in light fields simpler and more reliable. Tests and experimental verification of the constructed algorithms show that they are well adapted to the conditions of radiation propagation through randomly inhomogeneous media and allow, in combination with high-rate recording of interferograms, parameters of the probing beam to be estimated with the required accuracy

REFERENCES

1. A.S. Gurvich, A.I. Kon, V.L. Mironov, and S.S. Khmelevtsev, *Laser Radiation in a Turbulent Atmosphere* (Nauka, Moscow, 1976) [in Russian].
2. V.I. Tatarskii, "Atmospheric Turbulence and It Effect on Propagation of Electromagnetic Waves (Lecture)," in *Proceeding of the 1st All-Union School Symposium on Propagation of Millimeter and Submillimeter Waves in the Atmosphere* (10−17 February 1982, Moscow) (Moscow, 1983) [in Russian].
3. R. Bates and M. McDonnell, *Image Restoration and Reconstruction* (Clarendon, Oxford, 1989).
4. *Optical Shop Testing*, Ed. by D. Malacara (Wiley, N.Y., 1978).
5. E.G. Kim, A.M. Zotov, and N.L. Petrov, "Scaling Characteristics of Laser Beams in Randomly Inhomogeneous Media," Bull. Russ. Acad. Sci. Phys. **78**(12), 1260 (2014).
6. L.M. Soroko, *Hilbert Optics* (Nauka, Moscow, 1981) [in Russian].
7. M.A. Anan'in, and S.N. Khonina, "Modelling of Optical Processing of Images with Use of the Vortical Spatial Filter," Comp. Opt. **33**(4), 466 (2008) [in Russian].